A major hydrobiological change in Dasht-e Arjan Wetland (SW Iran) during the late glacial-early Holocene transition revealed by subfossil chironomids

Cyril Aubert[1*], Morteza Djamali[1,2], Matthew Jones[3], Hamid Lahijani[2], Nick Marriner[4], Abdolmajid Naderi-Beni [2], Arash Sharifi[5], Philippe Ponel[1], Emmanuel Gandouin[1]

1 CNRS, IRD, Aix Marseille Univ, Avignon Université, IMBE, Aix en Provence, France

2 INIOAS (Iranian National Institute for Oceanography and Atmospheric Sciences), No.3, Etemad Zadeh St., Fatemi Ave., Tehran, Iran, 1411813389, 14155-4781

3 School of Geography, University of Nottingham, University Park, Nottingham. NG7 2RD UK

4 Laboratoire de Chrono-Environnement, CNRS, Besançon, France

5 Halophytes and C4 Plants Research Laboratory, Department of Plant Science, School of Biology, University of Tehran, Tehran, Iran

***Corresponding author:** cyril.aubert@imbe.fr

Abstract

The late glacial-early Holocene transition is a key period in the Earth's history. However, although this transition is well studied in Europe, it is not well constrained in the Middle East and palaeohydrological records with robust chronologies remain scarce from this region. Here we present an interesting hydrobiological record showing a major environmental change occurring in the Dasht-e Arjan Wetland (SW Iran, near to Persepolis) during the late glacial-early Holocene transition (*ca*. 11,650 years cal BP). We use subfossil chironomids (Insecta: Diptera) as a proxy for hydrological changes and to reconstruct lake-level fluctuations. The Arjan wetland was a deep lake during the Younger Dryas (YD) marked by a dominance of *Chironomus plumosus/anthracinus*-type, taxa adapted to anoxic conditions of deep waters. At the beginning of the Holocene a drastic decrease (more than 80% to less than 10%) of *Chironomus plumosus/anthracinus*-type, combined with diversification of littoral taxa such as *Polypedilum nubeculosum*-type, *Dicrotendipes nervosus*-type and *Glyptotendipes pallens*-type suggest a lake-level decrease and a more vegetalized aquatic environment. We compare and contrast the chironomid record of Arjan with a similar record from northwestern Iran. The palaeoclimatic significance of the record, at a local and regional scale, is subsequently discussed. The increase in northern hemisphere temperatures, inferred by geochemical data from NGRIP, at the beginning of the Holocene best explains the change from the YD highstand to early Holocene lowstand conditions in the Dasht-e Arjan wetland. However, a contribution of the melt-water inflow from small local glaciers in the catchment basin is not excluded.

Key words: Younger Dryas, Climate change, Karst, Lake-level change, Zagros, late glacial-early Holocene transition, Iran, Middle East.

Introduction

The late Pleistocene to early Holocene transition marks the final part of the “Last Glacial-Interglacial Transition” (LGIT) or “Last Termination” (Lowe and Walker 1997; Hoek 2008). It is a key event in the Earth’s history characterized by a series of climatic changes of high magnitude that provide the possibility to investigate the mechanisms responsible for abrupt climatic changes (Hoek 2008). In the North Atlantic region, a detailed spatio-temporal framework is now available for the patterns of hydroclimatic and biotic changes during this transition (e.g. Ammann et al. 2000; Rasmussen et al. 2006). The biotic responses to late glacial-early Holocene climatic changes display many spatial discrepancies highlighting the important role of local ecological conditions such as lake topography and the composition of aquatic macrophyte communities (Engels and Cwynar, 2011). In the low temperate to subtropical latitudes of SW Asia, the late glacial hydroclimatic changes are still poorly understood compared to Europe and the Mediterranean. In the Middle East, for instance, the more complex interactions between climatic systems can potentially cause more multifaceted responses of biomes to hydroclimatic variations (Djamali et al. 2010). Furthermore, this is a key period during which nomadic hunter-gatherers sedenterized to form the first farming communities (Blockley and Pinhasi 2011; Willcox 2012). In this regard, the Zagros-Taurus Mountains in western Iran and southeastern Turkey is a key region in understanding the Neolithisation process (Matthews and Fazeli 2013). A recent discovery of the cultivation of wild cereals in the foothills of the Zagros Mountains in Iran (Riehl et al. 2013), at the very onset of the Holocene, suggests that this area should also be considered as one of the earliest centers for cereal and pulse domestication in the Middle East. In addition, the study of ancient DNA of human remains dating to Early Holocene suggests that the Zagros Mountains constitute the major center of eastward expansion of early farming communities (Broushaki et al. 2016). Unraveling the hydroclimatic changes associated with these events is thus important in understanding and in contextualizing the possible environmental changes responsible for the early Neolithisation of the region.

In the Middle East, although palaeohydrological records are available from NW Zagros, E Anatolia, Caucasus and the Talesh Mountains (e.g. Stevens et al. 2006; Sharifi et al. 2015; Aubert et al. 2017), no high-resolution record is available from the central-southern Zagros for the late glacial-early Holocene transition. The present study provides a hydrological record for this transition in the southern Zagros based on lacustrine deposits of the Dasht-e Arjan Wetland. Chironomid head capsules, which have been demonstrated to be good palaeo-temperature and palaeosalinity indicators (Heiri et al. 2011; Eggermont et al. 2006; Zhang et al. 2007), are also powerful proxies to reconstruct lake-level fluctuations (Eggermont et al. 2007). Recently, they have further been suggested as a promising proxy to reconstruct changes in precipitation seasonality in the semi-arid region of the Middle-East (Aubert et al. 2017). We place the new Arjan record in a regional context. We compare and contrast it with hydroclimatic changes of central Asia and Eastern Mediterranean, to further our regional understanding of ecosystem responses to this key climatic transition.

Materials and methods

Study area

Very little information is available from the wetland of Dasht-e Arjan (Plain of Arjan). The wetland (N 29°36’38”, E 51°59’04”, 1,984 m asl; Fig. 1) is located *ca*. 50 km to the west of Shiraz. It is a relatively large, moderately saline lake located near Lake Parishan with which it forms a Wetland of International Importance (Ramsar Site no. 37; https://www.ramsar.org). The climate of Shiraz (1,540 m asl) is of continental Mediterranean-type (Djamali et al. 2011) with most of the precipitation falling during the winter months (Fig 1C). Apart from the direct precipitation in its catchment basin, a major source for Dasht-e Arjan Wetland is the Arjan spring, which has a discharge rate fluctuating between 750 l/s and 100 l/s (Milanovic and Aghili 1990).

Although located within the Zagros Fold Belt, the Dasht-e Arjan region is situated in a local extensional tectonic setting which has created a subsiding sedimentary basin. The subsidence is controlled by the activity of two normal faults called the West Arjan Fault (N45°, 78°SE) and the East Arjan Fault (N55°, 70NW) which have created the 100-500 m high and ~10 km long SW-NE trended almost vertical cliffs composed mainly of Oligocene-Miocene Asmari Limestone formation to the west and east of the wetland (Fig. 1B; Seyrafian et al. 2011). Hydrogeologically, the Dasht-e Arjan Wetland seems to be located in a “polje” (a flat karstic plain) whose waters are evacuated through a “ponor” (an opening in the bottom of a polje), of 10-15 meter diameter, into a karstic subterraneous system during highstands with possible hydrological connection to the Kazerun (Lake Parishan) basin (Milanovic and Aghili 1990).

Fig. 1

Coring, lithostratigraphy and radiocarbon dating

Coring was performed using a Cobra vibracorer, allowing to gather 10 successive core sections of 1-m length and 5-cm width from the southeastern corner of the lake (29°35’33”N, 51°59’03”E, 1,992m asl) near the location of the “ponor” (Fig. 1B). The maximum depth attained was 960 cm. The lithostratigraphy comprises three major units: (1) a basal unit dominated by calcareous clayey mud with traces of pedogenesis; (2) middle section dominated by bioclastic calcareous mud; and (3) the upper unit dominated by organic-rich calcareous mud (Fig. 2; upper right). Six samples composed of bulk (peat and gyttja) and plant remains (fibers) were AMS radiocarbon dated at Poznan Radiocarbon Laboratory (Table 1). The radiocarbon ages were calibrated using Intcal13 calibration curve (Reimer et al. 2013) in the Clam package (Blaauw 2010) run in R software version 3.2.2 (R Core Team 2012). The age-depth model is based on linear interpolation taking into account the probability distribution of the calibrated ages (Fig. 2). Two radiocarbon ages were excluded from the age-depth model (sample Poz-Arj478 at 478 cm and sample Poz-Arj756 at 756 cm depth; Table 1). These two samples are outliers. The first sample is too old, possibly because of the old carbon found in the bulk sediment composed of calcareous mud, a sediment composition which tends to yield “older” ages (Table 1). The second sample is too young, most probably because it is composed of root and rootlets penetrating into old sediment from the much younger plants. The palustrine sedimentary facies which incorporates this sample display abundant root traces, corroborating this assumption (Fig. 2). A recent publication by Djamali et al. (2018) has shown that similar age inversions (too young ages) have also been reported from a palustrine carbonate facies in the western Persepolis basin. We have retained the ages provided by the samples Poz-Arj503, Poz-Arj614 and Poz-Arj671 because they are composed of *in situ* organic matter (gyttja to very fine grained peat), formed within the aquatic environments through biological processes. All carbonate content was removed through a chemical treatment at the radiocarbon laboratory of Poznan (T. Goslar, personal communication) diminishing the possible contamination by old carbon originating from geological formations. We consider that the age Poz-Arj614 giving a 2-σ range age of 11 631-12 060 is a very reliable age and marks the second part of the Younger Dryas, just before the onset of the Holocene. This age range is also displayed in the chironomid diagram of Fig. 3 (see discussion).

Chironomid analysis

Sixteen sediment samples weighing between 40 to 90 g were analyzed for chironomids, every 5 cm, along the fossiliferous interval of 630 to 550 cm. The laboratory methods used for extraction and identification of the chironomid subfossil head capsules are described in Gandouin et al. (2005). To summarize, the extraction consisted of KOH-deflocculation, water-washing over a 100 µm sieve and oil flotation. A minimum of 50 head capsules per sample is required to provide statistically significant estimates of ecological conditions (Heiri and Lotter 2001). Identification criteria of head capsules are based on a Palearctic dichotomous key developed by Brooks et al. (2007). The chironomid abundance diagram was created using C2 software version 1.7.2 (Juggins 2007).

Multivariate analyses of sub-fossil chironomid data

A constrained sum-of-squares cluster analysis (CONISS) for percentage data was performed with R (version 3.2.2) and the package “rioja” (Juggins 2017) to highlight major changes in chironomid assemblage composition throughout the stratigraphy (Grimm 1987). Principal Component Analysis (PCA) (Fig. 3) was performed on a data percentage matrix of 9 taxa for 16 samples. The PCA was carried out with “ade4” and “vegan” packages in R software (R Core Team 2012). Beforehand, data were square-root transformed with the aim of stabilizing the variance. Rare taxa (present in only one sample or with a relative abundance always <5 %) were excluded from analyses.

Results and interpretation

For the chironomid analysis, only the section between 630 and 550 cm was used because it corresponds to the late glacial-early Holocene transition and presents almost the only interval with sufficient chironomid head capsules for statistical analyses. Interestingly, this sequence of 0.80 meter corresponds to the end of the Younger Dryas and the onset of the Holocene (6.30-5.50 m: 12,380 to 10,103 years cal BP; Fig. 2). Fig. 3 presents a simplified diagram of chironomid relative abundances (in %). CONISS analysis revealed three faunal assemblage zones that we designate as Ach1: 630-605 cm (12,380-11,650 years cal BP), Ach2: 605-563 cm (~11,650-10,470 years cal BP) and Ach3: 563-555 cm (10,470-10,100 years cal BP). To the right of the chironomid diagram, percentage variations of a selection of pollen taxa have also been presented, based on a recently published pollen diagram from the same study core (Hosseini et al. 2017).

Fig. 2

Ach1: 630-605 cm (12,380-11,650 years cal BP):

This zone is dominated by *Chironomus plumosus*/*anthracinus*-type and significant presence of *Psectrocladius psilopterus*-type (Fig. 3). Together, these two chironomid taxa constitute up to 90% of the chironomid assemblage (Fig. 3). PCA scores for these chironomid taxa and the samples containing them are both positioned on the positive side of the PCA axis1 between 0.5 and 1 (Fig. 4).

The Ach1 upper boundary closely mirrors the ARJp1 pollen assemblage zone (Fig. 3, right panel). This pollen zone is characterized by the dominance of pollen produced by very dry steppe plants (Amaranthaceae, *Artemisia*) low values of *grasses* (Poaceae) and the total absence of trees. Only towards its end do aquatic plants (Cyperaceae) and algae increase (*Botryococcus* and *Pediastrum*).

Ach2: 605-563 cm (~11,650-10,470 years cal BP):

A remarkable faunal change occurs in this zone with a drastic reduction in *Chironomus plumosus*/*anthracinus*-type (Fig. 3) and, to a lesser extent, in *Psectrocladius psilopterus*-type percentages (from 80-90% to below 10% for the latter taxa). By contrast, other taxa such as *Polypedilum nubeculosum*-type, *Dicrotendipes nervosus*-type and *Glyptotendipes pallens*-type previously absent or in low abundances in the record, become the dominant chironomid assemblages. *Procladius* spp. percentages also increase during this zone. PCA axis1 scores follow the same trend as for *Chironomus plumosus*/*anthracinus*-type and decrease markedly to around -1 during most of the upper part of the zone (see Fig. 3).

Ach2 chironomid zone mostly correlates with ARJp2 pollen assemblage zone, characterized by a sudden drop and then low values of Amaranthaceae and the dominance of grasses and semi-continuous presence of aquatic plants (Cyperaceae and *Sparganium*-type) and algae (*Botryococcus* and *Pediastrum*). Tree pollen appear in the diagram although with low values. A treeless grass-dominated steppe with moderately developed aquatic vegetation is inferred (Hosseini et al., 2017).

Ach3: 563-555 cm (10,470-10,100 years cal BP):

During this zone, a slight rise of *Chironomus plumosus*/*anthracinus*-type and *Psectrocladius psilopterus*-type and a decrease of *Polypedilum nubeculosum*-type is observed (Fig. 3). Other littoral taxa such as *Dicrotendipes nervosus*-type and *Glyptotendipes pallens*-type are also present. Furthermore, we note the emergence of *Xenochironomus* spp. from 565 cm. During Ach3 zone, PCA axis1 scores increase slightly but remain negative (-0.5) at the top of sequence (Fig. 3).

Ach3 chironomid zone correlates with ARJp3 pollen assemblage zone in which grass pollen abundances decrease while Pediastrum shows a peak. At the regional scale, a dry mountain steppe vegetation and nutrient-rich mesotrophic conditions are inferred (based on *Pediastrum*).

Fig. 3

Statistically-based ecological groups of subfossil chironomids

PCA axis1 (56.2% of the total variance) opposes *Chironomus plumosus*/*anthracinus*-type on the positive side (Fig. 4) to *Glyptotendipes pallens*-type, *Procladius* spp., *Polypedilum nubeculosum*-type, *Tanytarsus* spp. and *Dicrotendipes nervosus*-type on the negative side. PCA axis 2 (17.3% of the total variance) is characterized by a segregation between *Xenochironomus* spp. and *Psectrocladius psilopterus*-type.

Fig. 4

Discussion

Chironomids as bathymetric bio-indicators

The PCA axis 1 clearly shows an opposition between *Chironomus plumosus*/*anthracinus*-type mostly confined to the profundal zone of lakes (Brooks et al. 2007) against the inhabitants of littoral zone and shallower water environments such as *Glyptotendipes pallens*-type and *Polypedilum nubeculosum*-type. *Glyptotendipes pallens*-type is most often associated with aquatic macrophytes (Brooks et al. 2007; Langdon et al. 2010). In fact, *Polypedilum nubeculosum*-type indicates relatively clear waters with variable macrophyte density and/or high plant species richness (Langdon et al. 2010). *Chironomus plumosus*/*anthracinus*-type are often associated with loose and fine-grained sediments such as mud and silt (Henrikson et al. 1982; Brodin 1986). Among the *Chironomus* genera, many species are also adapted to live and survive in deep waters, possibly hypoxic or anoxic conditions by producing a large amount of hemoglobin (Brooks et al. 2007). It is well established elsewhere that chironomids are influenced by lake bathymetry (Verneaux and Aleya 1998) and several transfer functions have been successfully developed to reconstruct Holocene lake-level changes in Scandinavia (Luoto et al. 2018), in Canada (Barley et al. 2006) and in China (Chang et al. 2017 and Wang et al. 2018).

Hence, PCA axis1 (Fig 4) may represent a bathymetric gradient with more positive scores indicating higher lake levels, whereas more negative scores indicate a shallower lake and marshy environments. Alternatively, the same trend may also indicate a transition from deep-water conditions to marsh environments that is not necessarily related to lake-level fluctuations but to the development of aquatic vegetation, from the littoral zone into the central lake basin. Either way, we consider the PCA axis1 scores as an indicator for lake-level changes for the Arjan wetland (Fig 3). In this way, we find a similar chironomid inferred hydrological dynamic already observed in Lake Neor (Fig. 5) located in northwestern Iran (Aubert et al. 2017). At this latter site, high wetland moisture indicating more permanent aquatic conditions are observed between 12,000 and 11,500 years cal BP. The wetland moisture became low between 11,500 and 10,300 years cal BP (Aubert et al. 2017) with the increase in semi-terrestrial taxa indicating ephemeral aquatic conditions on the lake margins.

The early Holocene section of our chironomid record shows a drastic fall in lake levels. This suggests a major environmental change in less than 100 years (Fig. 3 and 5); indeed, the Arjan wetland which was a deep lake during the Younger Dryas suddenly transformed into a shallow lake/marsh environment with a well-developed aquatic vegetation at the onset of the Holocene, from *ca.* 11,600 years (see aquatic pollen increase in Fig. 3). Increase of *Procladius* spp. is compatible with lower lake levels, since the members of this genus are carnivorous species (Brooks et al. 2007). In fact, in the shrinking lake water bodies, the higher prey concentration may favor the predation regime. Later, a decrease of *Polypedilum nubeculosum*-type and slight rise of *Chironomus plumosus*/*anthracinus*-type at the very end of our chironomid record suggest a slight increase in lake levels between 10,350-10,100 years cal BP. The persistence of other lacustrine littoral taxa e.g. *Psectrocladius psilopterus*-type., *Dicrotendipes nervosus*-type and *Glyptotendipes pallens*-type confirms the presence of a well-established aquatic vegetation, suggesting a relatively shallow lake/marsh environment. This notion is supported by higher total organic content (TOC), higher carbon accumulation rates and lower $\delta^{13}C_{TOC}$ at Lake Neor, NW Iran (Sharifi et al. 2015). The appearance of *Xenochironomus* spp. (Fig. 3) is imperatively associated with freshwater sponge (Pinder and Reiss 1983) also supporting the hypothesis of lake level increase during this period. Higher annual temperatures could explain the higher organic productivity in the Arjan wetland due to development of aquatic vegetation and its associated fauna (e.g. *Dicrotendipes nervosus*-type, *Glyptotendipes pallens*-type) at the very beginning of the Holocene.

Palaeoclimatic implications

In summary, the dominance of *Chironomus plumosus*/*anthracinus*-type indicates the presence of a deep and most probably stratified lake during Younger-Dryas in Dasht-e Arjan. Several hypotheses could explain such a highstand in Arjan during the YD:

(i) The intensity of the Siberian High during the YD was higher compared to the early Holocene (Mayewski et al. 1997; Sharifi et al. 2015). This would have pushed the westerlies to the south providing precipitation over the central and southern Zagros (Sharifi et al. 2018). However, YD pollen assemblages in Arjan are dominated by Amaranthaceae (Chenopodiaceae) with very low relative abundances of Poaceae (Fig. 3), indicating the presence of a typical dry steppe developed under a dry continental climate, exclude this first hypothesis.

(ii) Cooler summers during the YD in Northern Hemisphere could also explain higher moisture levels in both Arjan and Neor wetlands. Low YD temperatures would have decreased annual lake water evaporation. Evapo-transpiration was definitely lower under the generally colder temperatures of YD in southern Iran. Fig. 5 compares the chironomid-based lake-level variations of Arjan Wetland (right) with the NGRIP temperature record (North Greenland Ice Core Project members. 2004), and the Ti intensity curve, dust flux concentration curve and the chironomid-based lake-level variations in Lake Neor in northwestern Iran. It is interesting to note that the lake-level records in both Lake Neor and Arjan follow the same trend, which inversely correlates with NGRIP temperature record, suggesting the significance of low temperatures in maintaining high lake levels during the YD.

Fig. 5

(iii) Changes in the seasonality of precipitation, with increased rainfall during spring/summer months, could also lead to more permanent lake conditions during summer months (Aubert et al. 2017).

Indeed, late spring precipitation will permit maintaining higher lake levels during summer and greater humidity on lake margins. Nowadays, in the Arjan region, spring precipitation is lower than in northwestern Iran (Djamali et al. 2012) and regional palaeoclimatic records do not suggest increased spring/summer precipitation brought in by stronger monsoon conditions. They show that increased summer precipitation only began around 11,000 years cal BP peaking at 10,000-6,500 years cal BP and thus postdating the YD (Fleitmann et al. 2007). The hypothesis of a different precipitation seasonality is not satisfactory in explaining the high lake levels at Arjan during the YD.

(iv) A further hypothesis, is the presence of small glaciers in the catchment area of Arjan due to significant snowfall during the YD. Melt-waters would have maintained high lake levels during summers. Although no study has so far reported the glacier extensions in the area, the available studies on the last glacial maximum (LGM) glaciers in central Zagros suggest that the maximum descent of glaciers has been at around 2,400 m elevation during the LGM (Ebrahimi & Seif 2016). Presence of high mountains exceeding 2,600 m elevation in the lake catchment basin reinforces this hypothesis. Indeed, glaciers at higher elevations could lead to year-round inflow, or at least summer round inflow as they melt. This would be a distinct difference to Holocene conditions and would not necessitate a change in rainfall seasonality, but would change inflow seasonality. It may also explain why the lake levels fall after the transition to the Holocene, when all glaciers had already melted. A glacio-geomorphological survey to attest the evidence of glacier extension in the Arjan area would be helpful to investigate this. We therefore propose that a combination of lower evaporation due to lower annual temperatures, still significant precipitation due to the occasional penetration of southward-pushed westerlies into the southern Zagros (see Sharifi et al. 2018) and continuous glacier melting in the vicinity of the wetland could explain the high lake levels of Arjan during the YD.

(v) Finally, the hydroclimatic processes may not have been the only factor controlling the lake-level changes in Dasht-e Arjan. The complex karstic network of sinkholes in the southern part of the wetland basin could also have played a role in water-level fluctuations. Today, during the highstands, lake water is discharged through these karstic underground galleries preventing the lake level from exceeding a certain altitude corresponding to the sinkhole system in the southeast corner of the basin. The development of this karstic system and its connectivity to adjacent basins (e.g. Lake Parishan basin) possibly accelerated at the beginning of the Holocene. If such a hypothesis is correct, it can be proposed that the early Holocene lake levels would have been much higher if this karstic system had not developed. High-resolution lake level fluctuations at Lake Parishan during the YD-early Holocene may help to test this hypothesis e.g. by the detection of a synchronicity between the lake level fall in Arjan and a lake level rise in Parishan.

Whatever the case, the YD lake highstand in Arjan adds to the complex hydrological history of the Middle East at the late glacial-early Holocene transition. The hydrological history of each lake basin should be studied by taking into consideration a number of different factors of which climatic change constitutes just one component. For instance, comparing the hydrological evolution of two lake systems in central Anatolia, both located in the same climatic context and most probably experiencing the same hydroclimatic history, shows contrasting trends suggesting that climate was not the only factor controlling lake-level changes. Site-specific factors should also be taken into account when interpreting multi-proxy lake-level reconstructions (Roberts et al. 2016).

Dasht-e Arjan Wetland is located in a different climatic context compared to Anatolia and Europe from which numerous lake level reconstructions are available. Moreover, it would have possibly experienced a different climatic history due to its proximity to the monsoonal zone of southern Asia. It is not thus surprising that it presents a different late glacial-Holocene hydrological evolution when compared to the Eastern Mediterranean and Central Asia. Furthermore, as suggested by Roberts et al. (2016), more than one lake record is required to disentangle the changes related to climate change from those related to lake ontogeny. Before a general conclusion on lake hydrological changes in southern Zagros can be drawn, other lake records should thus be established and compared and contrasted with that of Arjan.

Southwest Asia shows a more complex hydroclimatic history compared to Europe, best exemplified by the ‘early Holocene precipitation paradox’. Indeed, the geochemical and pollen proxies suggest different hydrological regimes dominated during the early Holocene. While geochemical data suggest generally higher effective moisture, the pollen records indicate a limited expansion of deciduous forest and thus generally drier conditions. A number of hypotheses have been evoked by different scholars to explain this ‘paradox’ including a different precipitation seasonality in the early compared to the late Holocene, a strong early human impact on forest and steppe forest ecosystems, or a mixture of both (e.g. Stevens et al. 2001; Roberts 2002; Jones and Roberts 2008; Djamali et al. 2010). Part of such conflicting interpretations stems from the fact that the current interpretations are mainly based only on pollen and isotopic proxies. The new palaeohydrological indicators (fossil chironomid assemblages) presented in this study furnish additional data on lake-level changes and can help in explaining the hydrological paradoxes outlined above. The sensitivity of proxy records to local versus regional climate variabilities also needs to be investigated to supplement the high potential of chironomids, which may reflect changes in climate and hydrology at the local scale. The capacity of chironomid-based lake level reconstructions to detect high frequency events during the Holocene should therefore be evaluated in future palaeolimnological investigations.

Conclusions

The palaeoecological analysis of subfossil chironomid head capsules revealed a major change in the hydrology of Dasht-e Arjan Wetland at the transition of the Younger Dryas to the onset of the Holocene. In the absence of geochemical proxies from the studied sediment core, the chironomid data helped to reconcile the palaeohydrology of this low-latitude wetland situated in the southern Zagros Mountains. In the Zagros and adjacent highlands, although annual precipitation decreased in a similar manner as the rest of the Northern Hemisphere, the hydrological consequences of lower annual temperatures appear to have maintained higher amounts of water in the wetlands. During the YD, the possible contribution of melt-water from local glaciers to Arjan wetland hydrology shows the necessity to probe the late Quaternary history of glaciers in the Zagros Mountains. At present, it is unclear if such glaciers provided significant water resources during the late glacial period. More late glacial records are still required to understand the spatial patterns of hydrological change in the late Pleistocene-Holocene transition before a regional picture of the hydroclimatic mechanisms driving these changes can be drawn. Although the possible impacts of high effective moisture (high lake levels and aquifers) in the Iranian highlands on the early Neolithic communities was not discussed in the present paper, the data provided in this study, and similar investigations in the Fertile Crescent, will help to better understand the possible roles and explanatory mechanisms in the processes of Neolithisation. In particular, providing a palaeoenvironmental/palaeoclimate context for the beginning of plant/animal domestication and the establishment of the first Neolithic sedentary populations is extremely important.

The chironomid-based hydrological reconstruction from Lake Arjan is encouraging. In the future, more quantified data are required for comparisons with regional palaeoclimatic records e.g. the Sea Surface Temperatures of the Arabian Sea or the speleothem records from Southern Asia, Northern Iran, Arabia, and Turkey.

Acknowledgments

We wish to thank the Agence Nationale de Recherche (ANR) as well as the Centre National de la Recherche Scientifique (CNRS) for their financial support of this study under the Franco-German ANR/DFG project “PALEOPERSEPOLIS’’ (ANR-14-CE35-0026-01) and the Franco-Iranian International Associated Laboratory project called “HAOMA”. We also thank Marine Leteurtrois and Gwenaël Magne for their assistance in data acquisition. We wish to thank Professors Neil Roberts (Plymouth University) and Lora Stevens (California State University at Long Beach) for their helpful comments on the interpretation of our data. Finally, we extend our gratitude to two anonymous reviewers for their thoughtful and constructive comments on an earlier version of this paper.

Reference

Aubert, C., .Brisset, E., Djamali, M., Sharifi, A., Ponel, P., Gambin, B., Akbari- Azirani, T., Guibal, F., Lahijani, H., Naderi-Beni, A., de Beaulieu, J.-L., Pourmand, A., Andrieu-Ponel, V., Thiéry, A., and Gandouin, E. 2017. Late glacial and early Holocene hydroclimate variability in northwest Iran (Talesh Mountains) inferred from chironomid and pollen analysis. Journal of Paleolimnology, **58**: 151–167.

Ammann, B., Birks, H.J., Brooks, S.J., Eicher, U., von Grafenstein, U., Hofmann, W., Lemdahl, G., Schwander, J., Tobolski, K., and Wick, L. 2000. Quantification of biotic responses to rapid climatic changes around the Younger Dryas - a synthesis. Palaeogeography, Palaeoclimatology, Palaeoecology, **159**: 313–347.

Barley, E.M., Walker, I.R., Kurek, J., Cwynar, L.C., Mathewes, R.W., Gajewski, K., and Finney, B.P. 2006. A northwest North American training set: distribution of freshwater midges in relation to air temperature and lake depth. Journal of Paleolimnology, **36**: 295–314.

Blaauw, M. 2010. Methods and code for 'classical' age-modelling of radiocarbon sequences. Quaternary geochronology, **5**: 512–518.

Blockley, S.P.E., and Pinhasi, R. 2011. A revised chronology for the adoption of agriculture in the Southern Levant and the role of Lateglacial climatic change. Quaternary Science Reviews, **30**: 98–108.

Brodin, Y.W. 1986. The postglacial history of Lake Flarken, southern Sweden, interpreted from subfossil insect remains. Internationale Revue der Gesamten Hydrobiologie, **71**: 371–432.

Brooks, S.J., Langdon, P.G., and Heiri, O. 2007. The identification and Use of Palaeartic Chironomidae Larvae in Palaeoecology. Technical Guide N°10. Quaternary Research Association, London.

Broushaki, F., Thomas, M.G., Link, V., López, S., van Dorp, L., Kirsanow, K., Hofmanová, Z., Diekmann, Y., Cassidy, L.M., and Díez-del-Molino, D. 2016. Early Neolithic genomes from the eastern Fertile Crescent. Science, **353**: 499–503.

Chang, J., Zhang, E., Liu, E., and Shulmeister, J. 2017. Summer temperature variability inferred from subfossil chironomid assemblages from the south-east margin of the Qinghai–Tibetan Plateau for the last 5000 years. The Holocene, **27**: 1876–1884.

Djamali, M., Akhani, H., Andrieu-Ponel, V., Braconnot, P., Brewer, S., Beaulieu, J.-L., Fleitmann, D., Fleury, J., Gasse, F., Guibal, F., Jackson, S.T., Lézin,e A.-M., Médail, F., Ponel, P., Roberts, N., and Stevens, L. 2010.

Indian Summer Monsoon variations could have affected the early-Holocene woodland expansion in the Near East. The Holocene, **20**: 813–820.

Djamali, M., Akhani, H., Khoshravesh, R., Andrieu-Ponel, V., Ponel, P., and Brewer, S. 2011. Application of the global bioclimatic classification to Iran: implications for understanding the modern vegetation and biogeography. Ecologia Mediterranea, **37**: 91–114.

Djamali, M., Baumel, A., Brewer, S., Jackson, S.T., Kadereit, J.W., López-Vinyallonga, S., Mehregan, I., Shabanian, E., and Simakova, A. 2012. Ecological implications of Cousinia Cass. (Asteraceae) persistence through the last two glacial–interglacial cycles in the continental Middle East for the Irano-Turanian flora. Review of Palaeobotany and Palynology, **172**: 10–20.

Djamali, M., Gondet, S., Ashjari, J., Marriner, N., Aubert, C., Brisset, E., Longerey, J., Mashkour, M., Miller, N.F., Naderi-Beni, A., Pourkerman, M., Rashidian, E., Rigot, J.-B., Shidrang, S., Thiéry, A., and Gandouin, E. 2018. Karstic-spring wetlands of the Persepolis Basin, SW Iran: unique sediment archives of Holocene environmental change and human impacts. Canadian Journal of Earth Science. doi/10.1139/cjes-2018-0065.

Ebrahimi, B., and Seif, A. 2016. Equilibrium-Line Altitudes of Late Quaternary Glaciers in the Zardkuh Mountain. Geopersia, **6(2)**: 299-322.

Eggermont, H., Heiri, O., and Verschuren, D. 2006. Fossil Chironomidae (Insecta: Diptera) as quantitative indicators of past salinity in African lakes. Quaternary Science Reviews, **25**: 1966–1994.

Eggermont, H., De Deyne, P., and Verschuren, D. 2007. Spatial variability of chironomid death assemblages in the surface sediments of a fluctuating tropical lake (Lake Naivasha, Kenya). Journal of Paleolimnology, **38**: 309–328.

Engels, S., and Cwynar, L.C. 2011. Changes in fossil chironomid remains along a depth gradient: evidence for common faunal thresholds within lakes. Hydrobiologia 665, 15–38.

Fleitmann, D., Burns, S.J., Mangini, A., Mudelsee, M., Kramers, J., Villa, I., Neff, U., Al-Subarry, A., Buettner, A., Hippler, D., and Matter, A. 2007. Holocene ITCZ and Indian monsoon dynamics recorded in stalagmites from Oman and Yemen (Socotra). Quaternary Science Reviews, **26**: 170–188.

Gandouin, E., Franquet, E., and Van Vliet-Lanoe, B. 2005. Chironomids (Diptera) in River Floodplains: their Status and Potential Use for Palaeoenvironmental Reconstruction Purposes. Archiv für Hydrobiologie, **162**: 511–534.

Grimm, E.C. (1987) CONISS: A FORTRAN 77 program for stratigraphically constrained cluster analysis by the method of incremental sum of squares. Computers & Geosciences, **13**: 13–35.

Heiri, O., Brooks, S.J., Birks, H.J.B., and Lotter, A.F. 2011. A 274-lake calibration dataset and inference model for chironomid-based summer temperature reconstruction in Europe. Quaternary Science Reviews, **30**: 3445–3456.

Heiri, O., and Lotter, A.F. 2001. Effect of low count sums on quantitative environmental reconstructions: an example using subfossil chironomids. Journal of Paleolimnology, **26**: 343–350.

Henrikson, L., Olofsson, J.B., and Oscarson, H.G. 1982. The impact of acidification on Chironomidae (Diptera) as indicated by subfossil stratification. Hydrobiologia, **86**: 223-229.

Hoek, W.Z., Yu, Z.C., and Lowe, J.J. 2008. INTegration of Ice-core, MArine, and TErrestrial records (INTIMATE): refining the record of the Last Glacial–Interglacial Transition. Quaternary Science Reviews, **27**: 1–5.

Hosseini, Z., Khaledi, S., and Naderi-Beni, A. 2017. Reconstruction of vegetation and palaeoclimate of Dasht-e Arjan, Fars, during the late Pleistocene and Holocene based on pollen analysis. Journal of climatological studies, **27-28**: 87–98 (paper in Persian language).

Jones, M. D., and Roberts, C. N. 2008. Interpreting lake isotope records of Holocene environmental change in the Eastern Mediterranean. Quaternary International, **181**: 32–38.

Juggins, S. 2007. C2 Version 1.5 User guide. Software for ecological and palaeoecological data analysis and visualisation. NewcastleUniversity, Newcastle upon Tyne, UK. 73pp.

Juggins, S. (2017) rioja: Analysis of Quaternary Science Data, R package version (0.9-15.1). (http://cran.r-project.org/package=rioja).

Langdon, P., Ruiz, Z., Wynne, S., Sayer, C., and Davidson, T. 2010. Ecological influences on larval chironomid communities in shallow lakes: implications for palaeolimnological interpretations. Freshwater Biology, **55**: 531–545.

Lowe, J.J., and Walker, M.J.C. 1997. Reconstructing Quaternary Environments, 2 edition. ed. Routledge, Harlow.

Luoto, T.P., Ojala, A.E.K., Arppe, L., Brooks, S.J., Kurki, E., Oksman, M., Wooller, M.J., and Zajączkowski, M. 2018. Synchronized proxy-based temperature reconstructions reveal mid- to late Holocene climate oscillations in High Arctic Svalbard. Journal of Quaternary Science, **33**: 93–99.

Matthews, R., and Fazeli Nashli, H. 2013. The neolithisation of Iran. Oxbow Books. Oxford (Royaume Uni).

Mayewski, P.A., Meeker, L.D., Twickler, M.S., Whitlow, S., Yang, Q., Lyons, W.B., and Prentice, M. 1997. Major features and forcing of high254 P.A. Mayewski et al. / Quaternary Research 62 (2004) 243–255 latitude northern hemisphere atmospheric circulation using a 110,000- year long glaciochemical series. Journal of Geophysical Research, **102**: 26345–26366.

Milanovic, P., and Aghili, B. 1990. Hydrogeological characteristics and groundwater mismanagement of kazerun karstic aquifer, Zagros, Iran. Hydrogeological Processes in Karst Terranes, **10**: 163–171.

North Greenland Ice Core Project members. 2004. High-resolution record of Northern Hemisphere climate extending into the last interglacial period. Nature, **431(7005)**: 147–151.

Pinder, L.C.V., and Reiss, F. 1983. The Larvae of Chironominae (Diptera: Chironomidae) of the Holartic region. Keys and diagnoses. Entomol Scand Supplement, **19**: 293–435.

R Core Team 2012. R: A language and environment for statistical computing. R Foundation for Statistical Computing, Vienna, Austria.

Rasmussen, S.O., Andersen, K.K., Svensson, A.M., Steffensen, J.P., Vinther, B.M., Clausen, H.B., Siggaard-Andersen, M.-L., Johnsen, S.J., Larsen, L.B., Dahl-Jensen, D., Bigler, M., Rothlisberger, R., Fischer, H., Goto-Azuma, K., Hansson, M.E., and Ruth, U. 2006. A new Greenland ice core chronology for the last glacial termination. Journal of Geophysical Research, **111**. doi:10.1029/2005JD006079.

Reimer, P.J., Bard, E., Bayliss, A., Beck, J.W., Blackwell, P.G., Ramsey, C.B., Buck, C.E., Cheng, H., Edwards, R.L., Friedrich, M., Grootes, P.M., Guilderson, T.P., Haflidason, H., Hajdas, I., Hatté, C., Heaton, T.J., Hoffmann, D.L., Hogg, A.G., Hughen, K.A., Kaiser, K.F., Kromer, B., Manning, S.W., Niu, M., Reimer, R.W., Richards, D.A., Scott, E.M., Southon, J.R., Staff, R.A., Turney, C.S.M., and van der Plicht, J. 2013. IntCal13 and Marine13 Radiocarbon Age Calibration Curves 0–50,000 years cal BP. Radiocarbon, **55**: 1869–1887.

Riehl, S., Zeidi, M., and Conard, N.J. 2013. Emergence of Agriculture in the Foothills of the Zagros Mountains of Iran. Science, **341**: 65–67.

Roberts, N. 2002. Did prehistoric landscape management retard the post-glacial spread of woodland in Southwest Asia? Antiquity, **76**: 1002–1010.

Roberts, N., Allcock, S.L., Arnaud, F., Dean, J.R., Eastwood, W.J., Jones, M.D., Leng, M.J., Metcalfe, S.E., Malet, E., Woodbridge, J., and Yiğitbaşıoğlu, H. 2016. A tale of two lakes: a multi-proxy comparison of Lateglacial and Holocene environmental change in Cappadocia, Turkey: A TALE OF TWO LAKES. Journal of Quaternary Science, **31**: 348–362.

Seyrafian, A., Vaziri-Moghaddam, H., Arzani, N., and Taheri, A. 2011. Facies analysis of the Asmari Formation in central and north-central Zagros basin, southwest Iran: Biostratigraphy, paleoecology and diagenesis. Revista Mexicana de Ciencias Geológicas, **28(3)**: 439–458.

Sharifi, A., Pourmand, A., Canuel, E.A., Ferer-Tyler, E., Peterson, L.C., Aichner, B., Feakins, S.J., Daryaee, T., Djamali, M., Beni, A.N., Lahijani, H.A.K., and Swart, P.K. 2015. Abrupt climate variability since the last deglaciation based on a high-resolution, multi-proxy peat record from NW Iran: The hand that rocked the Cradle of Civilization? Quaternary Science Reviews, **123**: 215–230.

Sharifi, A., Murphy, L.N., Pourmand, A., Clement, A.C., Canuel, E.A., Naderi Beni, A., A.K. Lahijani, H., Delanghe, D., and Ahmady-Birgani, H. 2018. Early-Holocene greening of the Afro-Asian dust belt changed sources of mineral dust in West Asia. Earth and Planetary Science Letters, **481**: 30–40.

Stevens, L.R., Wright, H.E. Jr., and Ito, E. 2001. Proposed changes in seasonality of climate during the Lateglacial and Holocene at Lake Zeribar, Iran. The Holocene, **11**: 747–755.

Stevens, L.R., Ito, E., Schwalb, A., and Wright, H.E. Jr. 2006. Timing of atmospheric precipitation in the Zagros Mountains inferred from a multi-proxy record from Lake Mirabad, Iran. Quaternary Research, **66**: 494–500.

Verneaux, V., and Aleya, L. 1998. Bathymetric distributions of chironomid communities in ten French lakes: Implications on lake classification. Fundamental and Applied Limnology, **142**: 209–228.

Wang, H., Chen, J., Zhang, S., Zhang, D.D., Wang, Z., Xu, Q., Chen, S., Wang, S., Kang, S., and Chen, F. 2018. A chironomid-based record of temperature variability during the past 4000 years in northern China and its possible societal implications. Climate of the Past, **14**: 383–396.

Willcox, G. 2012. The beginnings of cereal cultivation and domestication in Southwest Asia. In D. Potts (ed.) A companion to the archaeology of the ancient Near East. Wiley Blackwell Malden, Oxford.

Zhang, E., Jones, R., Bedford, A., Langdon, P., and Tang, H. 2007. A chironomid-based salinity inference model from lakes on the Tibetan Plateau. Journal of Paleolimnology, **38**: 477–491.

Table:

Table 1. ^{14}C ages obtained and the type of corresponding material (Lake Arjan). Calibrated ages are reported with 2-σ ranges. Excluded ages are marked in *italics*.

Laboratory code	**Depth (cm)**	**Material**	**Age years BP (^{14}C)**	**Age years cal BP (2σ interval)**
Poz-Arj148	148	Organic mud	6430 ± 50	7356 (7274-7429)
Poz-Arj478	*478*	*Calcareous mud (bulk)*	*9280 ± 50*	*10455 (10287-10612)*
Poz-Arj503	503	Gyttja (bulk)	7940 ± 50	10715 (10573-10844)
Poz-Arj614	614	Gyttja (bulk)	10180 ± 50	11869 (11631-12060)
Poz-Arj671	671	Gyttja (bulk)	11880± 60	12408 (12255-12536)
Poz-*Arj756*	*756*	Plant remains	*11370*± 60	*13212* (13099-13332)

Figure captions:

Figure 1: A. Location of Dasht-e Arjan Wetland and Lake Neor in Iranian plateau. B. The fault system controlling the subsidence of the Arjan Basin with the position of the coring site. C. Climate diagram of Shiraz. D. Dasht-e Arjan during a lowstand with the position of coring site (Source: Google Earth; Landsat/Copernicus (B dating to 12/1987) and CNES/Airbus (C dating to 12/2016)).

Figure 2. Lithostratigraphic log and age-depth model for the whole core (upper right) with a detailed focus on the studied section from Dasht-e Arjan Wetland. The chironomid record presented here corresponds to the depths of 630 to 550 cm (12 000 to 11 200 years cal BP).

Figure 3. Synthetic subfossil chironomid diagram from the Lake Arjan record (left) compared to pollen records for the same section of the same core (see Hosseini et al., 2017 for a detailed pollen diagram). The zonation pollen diagram was made visually. Profundal taxa: inhabit profundal zones of lake. Littoral taxa: inhabit littorals margins of lake. Other taxa: indifferent to depth or no documented ecological affinities.

Figure 4. Scatter plots for PCA scores of chironomid assemblages in the late glacial-Early Holocene transition sediments of Dasht-e Arjan Wetland core showing the variable factor map of PCA (A) and contribution of different variables (taxa) to axis 1 (B) and axis 2 (C).

Figure 5. Comparison of the abundance of the sum of the deep water chironomid taxa between Lake Arjan and Lake Neor (Aubert et al. 2017) compared with temperature variations in Greenland (NGRIP record: North Greenland Ice Core Project members (2004) and aeolian activity in Lake Neor (Sharifi et al. 2015).

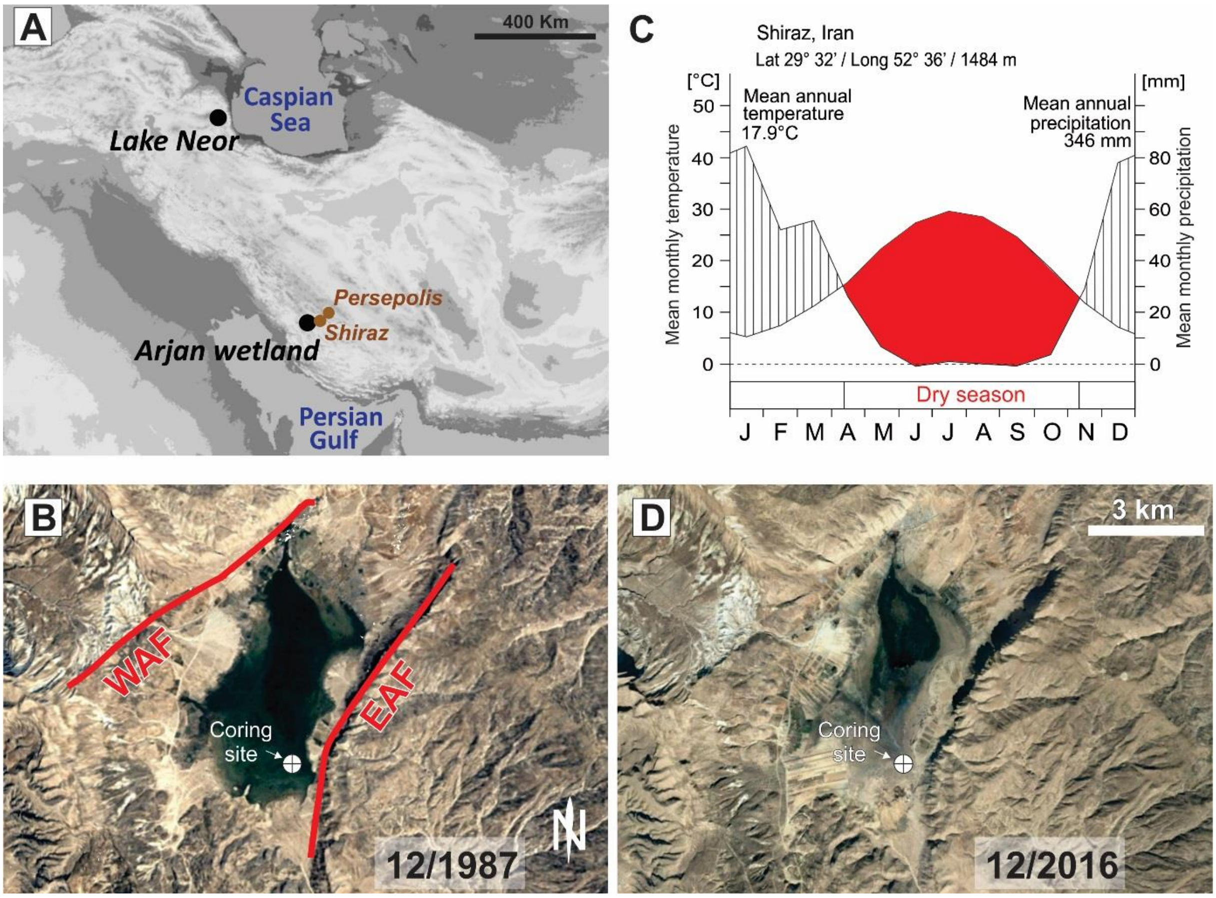
A
400 Km
Caspian Sea
Lake Neor
Persepolis
Shiraz
Arjan wetland
Persian Gulf
C
Shiraz, Iran
Lat 29° 32' / Long 52° 36' / 1484 m
[°C]
[mm]
Mean annual temperature 17.9°C
Mean annual precipitation 346 mm
Mean monthly temperature
Mean monthly precipitation
50
40
30
20
10
0
80
60
40
20
0
Dry season
J F M A M J J A S O N D
B
WAF
EAF
Coring site
12/1987
D
3 km
Coring site
12/2016

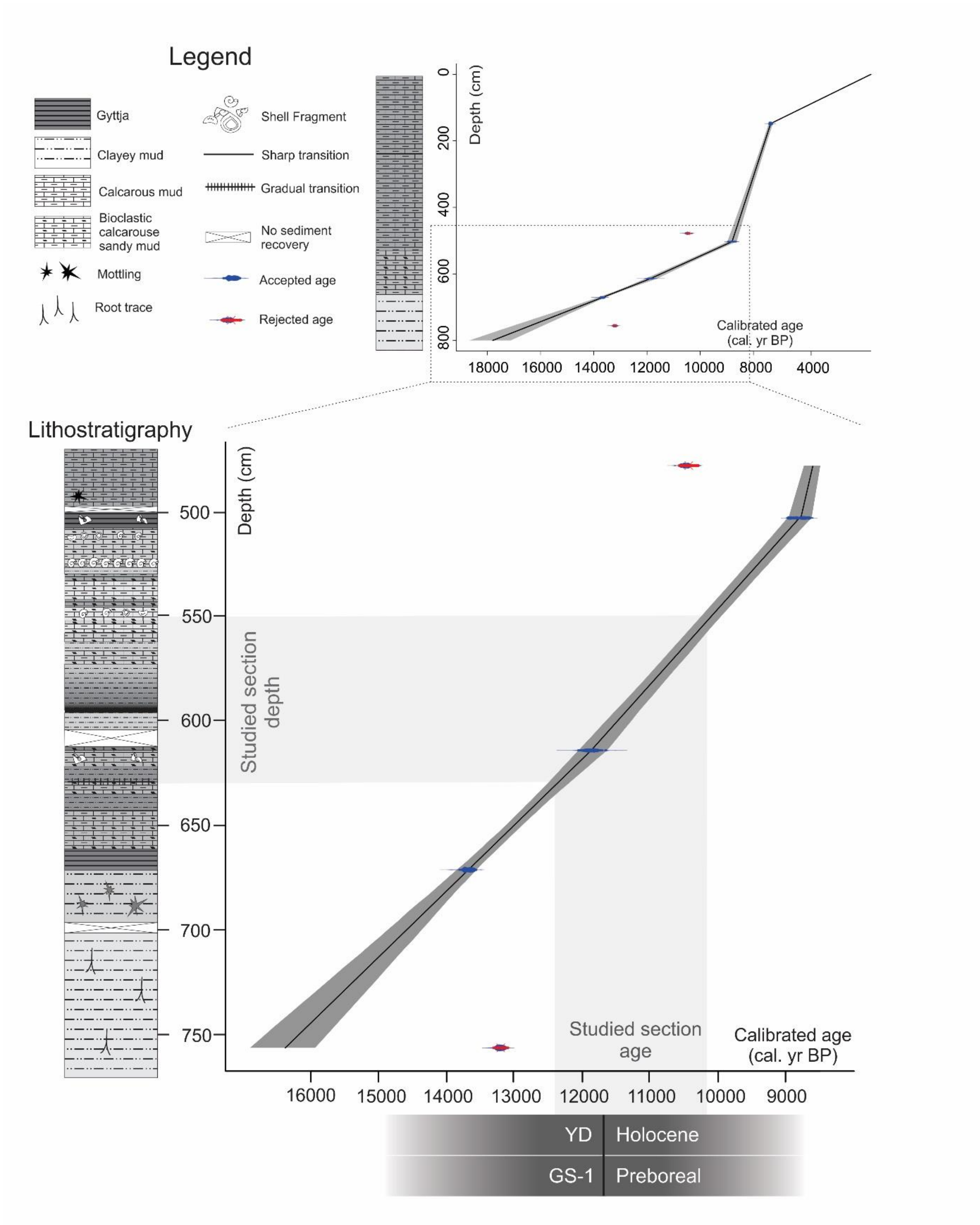

Legend
Gyttja
Clayey mud
Calcarous mud
Bioclastic calcarouse sandy mud
Mottling
Root trace
Shell Fragment
Sharp transition
Gradual transition
No sediment recovery
Accepted age
Rejected age
Depth (cm)
0
200
400
600
800
Calibrated age (cal. yr BP)
18000
16000
14000
12000
10000
8000
4000
Lithostratigraphy
Depth (cm)
500
550
600
650
700
750
Studied section depth
Studied section age
Calibrated age (cal. yr BP)
16000
15000
14000
13000
12000
11000
10000
9000
YD
Holocene
GS-1
Preboreal

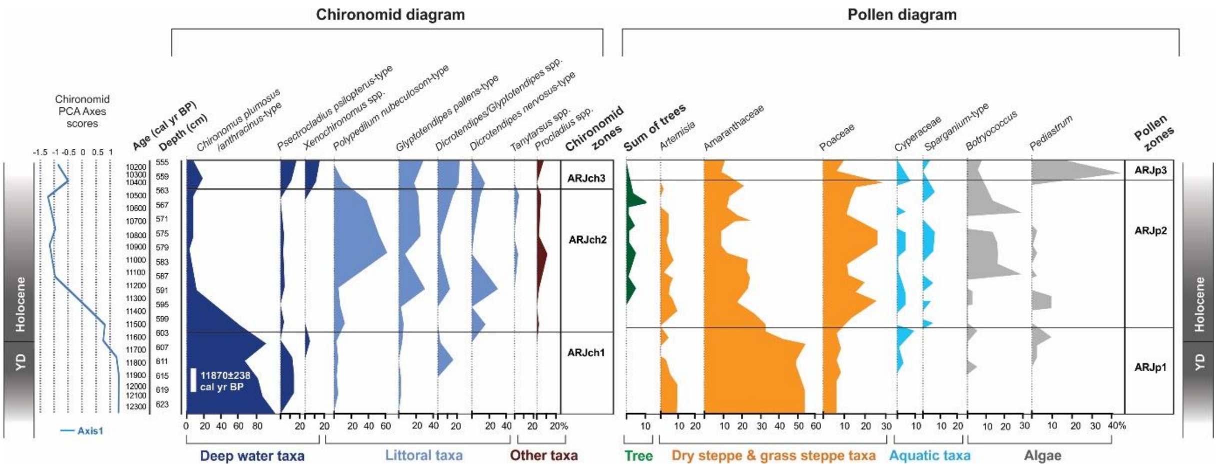
Chironomid diagram
Pollen diagram
Chironomid PCA Axes scores
Age (cal yr BP)
Depth (cm)
Chironomus plumosus /anthracinus-type
Psectrocladius psilopterus-type
Xenochironomus spp.
Polypedilum nubeculosom-type
Glyptotendipes pallens-type
Dicrotendipes/Glyptotendipes spp.
Dicrotendipes nervosus-type
Tanytarsus spp.
Procladius spp.
Chironomid zones
Sum of trees
Artemisia
Amaranthaceae
Poaceae
Cyperaceae
Sparganium-type
Botryococcus
Pediastrum
Pollen zones
ARJch3
ARJch2
ARJch1
ARJp3
ARJp2
ARJp1
Holocene
YD
11870±238 cal yr BP
Axis1
Deep water taxa
Littoral taxa
Other taxa
Tree
Dry steppe & grass steppe taxa
Aquatic taxa
Algae

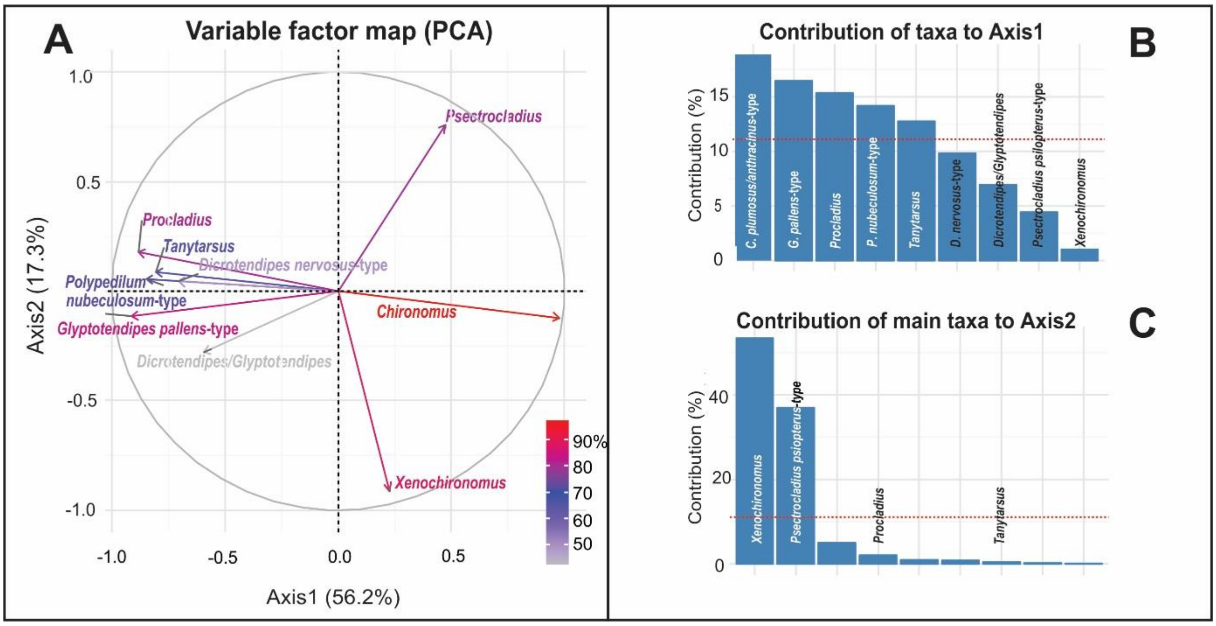

A
Variable factor map (PCA)
Psectrocladius
Procladius
Tanytarsus
Dicrotendipes nervosus-type
Polypedilum
nubeculosum-type
Chironomus
Glyptotendipes pallens-type
Dicrotendipes/Glyptotendipes
Xenochironomus
Axis2 (17.3%)
Axis1 (56.2%)
1.0
0.5
-0.5
-1.0
0.0
90%
80
70
60
50
B
Contribution of taxa to Axis1
Contribution (%)
15
10
5
0
C. plumosus/anthracinus-type
G. pallens-type
Procladius
P. nubeculosum-type
Tanytarsus
D. nervosus-type
Dicrotendipes/Glyptotendipes
Psectrocladius psilopterus-type
Xenochironomus
C
Contribution of main taxa to Axis2
40
20
Xenochironomus
Psectrocladius psiopterus-type
Procladius
Tanytarsus

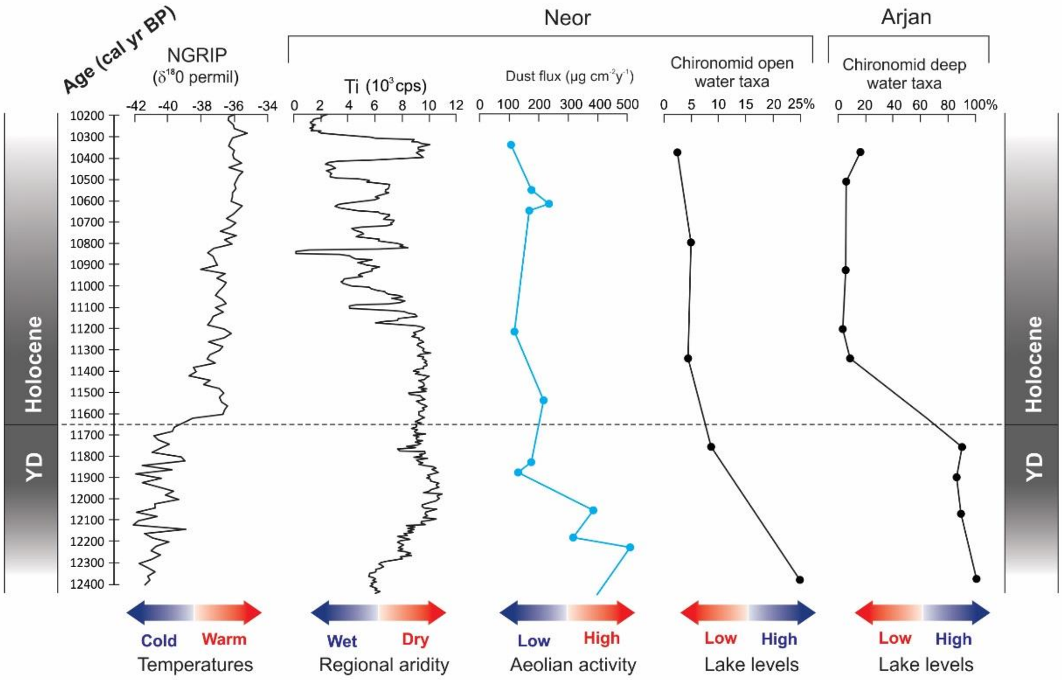

Age (cal yr BP)
NGRIP
(δ18O permil)
Neor
Arjan
Ti (10³cps)
Dust flux (μg cm⁻²y⁻¹)
Chironomid open water taxa
Chironomid deep water taxa
Holocene
YD
Cold Warm
Temperatures
Wet Dry
Regional aridity
Low High
Aeolian activity
Low High
Lake levels
Low High
Lake levels

548